Observation of Gravity Waves from Space
CN/22561/09/NL/AF

Executive Summary

November 2012

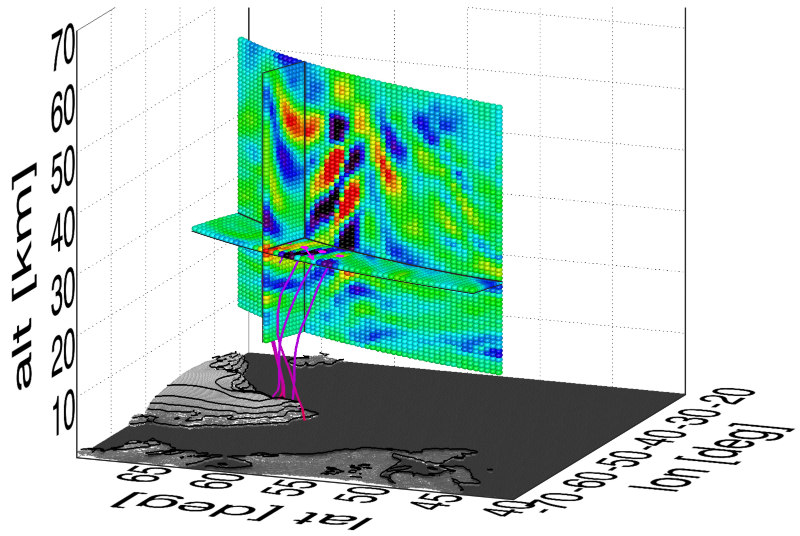

Peter Preusse[1], Lars Hoffmann[1,2], Catrin Lehmann[1], M. Joan Alexander[3], Dave Broutman[4], Hye-Yeong Chun[5], Anu Dudhia[6], Albert Hertzog[7], Michael Höpfner[8], Young-Ha Kim[5], William Lahoz[9], Jun Ma[4], Manuel Pulido[10], Martin Riese[1], Harjinder Sembhi[11], Sabine Wüst[12], Verena Alishahi[1], Michael Bittner[12], Manfred Ern[1], Pier Giuseppe Fogli[13], So-Young Kim[5], Verena Kopp[12], Magdalena Lucini[10], Elisa Manzini[14], John C. McConnell[15], Juan Ruiz[10], Guillermo Scheffler[10], Kirill Semeniuk[15], Viktoria Sofieva[16], and François Vial[7]

1) Institut für Energie und Klima (IEK-7), Forschungszentrum Jülich, 2) Jülich Supercomputing Centre (JSC), Forschungszentrum Jülich, 3) CoRA Division, North West Research Associates, 4) Computational Physics Incorporated, 5) Department of Atmospheric Sciences, Yonsei University, 6) Atmospheric, Oceanic and Planetary Physics, University of Oxford, 7) Laboratoire de Météorologie Dynamique, CNRS, 8) Institut für Meteorologie und Klima, Karlsruhe Institute of Technology, 9) NILU, 10) Dept. of Physics, FACENA, Universidad Nacional del Nordeste, 11) Earth Observation Science, Space Research Centre, University of Leicester, 12) Deutsches Fernerkundungsdatenzentrum, Deutsches Zentrum für Luft-und Raumfahrt, 13) Centro Euro-Mediterraneo per i Cambiamenti Climatici, Bologna, Italy 14) Max-Planck-Institut für Meteorologie, Hamburg, Germany, 15) CRESS, Centre for Research in Earth and Space Science, York University, 16) Finnish Meteorological Institute,

1 Background to the study

This study was commissioned by ESA following selection of PREMIER by ESA's PB-EO in February 2009 for feasibility studies (Phase A) as one of three candidate missions for Earth Explorer-7. The purpose of the study was to demonstrate that an infrared limb imager as to be used in the PREMIER mission is able to quantify gravity wave (GW) momentum flux at an accuracy sufficient to solve open scientific questions in this field. In particular, it shall be demonstrated that PREMIER can provide unprecedented information on the global momentum budget as well as on various GW processes and that comparable information cannot be obtained by any other measurement technique which could be realized by current technology.

The gravity wave study is one of several studies in support of the mission including the Consolidation of Requirements and Synergistic Retrieval Algorithms (CORSA), the "Science Impact Study" and two airborne campaigns deploying precursor instruments on the high-altitude research aircraft Geophysika.

The study was extensive in scope and organized in the following tasks

1. Literature study and definition of requirements
2. Selection of numerical models and scenarios
3. PREMIER 2D temperature retrieval
4. Tools for GW isolation and identification
5. Gravity wave ray tracing
6. Determination and assessment of GW momentum flux
7. Scientific interpretation by ray tracing
8. Validation
9. Conclusions and recommendations

To accomplish these Tasks a consortium of scientific groups was assembled to cover the required range of expertise, with the following division of responsibilities:

Forschungszentrum Jülich, Germany

- Prime contractor
- Literature study
- Selection of scenarios
- Generation of PREMIER simulated orbit and measurement geometry
- Setup of 2D retrieval system
- Execution of radiative transfer and retrieval simulation
- Isolation of GWs from global scale background
- GW characterization tool
- Quantitative assessment of the momentum flux accuracy
- Backward ray tracing for GW source identification

University of Oxford, UK

- Selection of optimized spectral micro windows for retrievals
- Retrieval error estimations

University of Leicester, UK

- Generation of a climatology including characterization of the variability of temeperatures and trace species for the training of the retrievals

Karlsruhe Institute of Technology, Germany

- Performance of radiative transfer simulations
- Validation of the 2D retrieval system

Computational Physics Incorporated, USA

- Literature study
- Numerical and mathematical studies to the theoretical background
  (validity of e.g. polarization relations in cases of violation of the WKB approximation)
- Performance of mountain wave simulations

Laboratoire de Meteorologie Dynamique, France

- Literature study
- Development of the validation concept

Deutsches Zentrum für Luft- und Raumfahrt, Germany

- Contributions to GW analysis
- Contributions to validation concept

NILU, Norway

- Literature study
- Role of data assimilation for validation and scientific interpretation

Yonsei University, Korea

- Simulation of convective GWs
- Validation of the GW characterization method

Universidad Nacional del Nordeste, Argentinia

- Simulation of mountain waves
- Role of data assimilation for validation and scientific interpretation

Colorado Research Associates, USA

- Simulation of convective GWs
- Global relevance of GWs

York University, Canada

- Simulation of convective GWs
- Simulation of mountain waves

Finnish Meteorological Institute, Finland

- Contributions to validation concept

In addition, we thank Elisa Manzini and Pier Giuseppe Fogli for providing data from the ECHAM general circulation model (GCM). These data were generated in the frame of a work-group on "Merging space- and ground-based observational constraints for gravity wave parameterizations in climate models" supported by the International Space Science Institute (ISSI; http://www.issibern.ch/teams/gravitywave/index.html). We also thank the members of the ISSI team for discussions and support of the mission.

2 General overview: aim and outline of simulations

Gravity waves can exist in a stably stratified medium in the presence of gravity. They are important dynamical drivers in the ocean, the sun and planetary atmospheres. In this study we focus on the impact and measurement of gravity waves in Earth's middle atmosphere, the region accessible by PREMIER. Atmospheric gravity waves (GWs) are waves in temperature, density and winds with the restoring force of buoyancy or gravity. They propagate upward from mostly tropospheric sources and convey momentum from low to higher altitudes thus coupling the different layers of the atmosphere. The key quantity which needs to be measured is therefore the momentum flux conveyed by the observed gravity waves (in short GW momentum flux or GWMF). We will highlight some important phenomena generated by GW coupling in section 3. A basic introduction of GW physics is given in the final report, review papers on GWs and their impact include *Fritts* (1984); *McLandress* (1998); *Fritts and Alexander* (2003); *Kim et al.* (2003); *Alexander et al.* (2010).

Despite a long-standing research, many questions on GWs are unsolved. The chief problem is the interaction of different scales. While the effects of GWs are global, their excitation involves, for instance, the details of convection and wave breaking and requires, if to be modeled accurately, resolutions of 100 m in the horizontal or finer (*Lane and Knievel*, 2005). It is therefore essential to measure the momentum flux by GWs globally, that is by satellites. Based on work on existing satellite measurements (e.g. *Ern et al.*, 2004), in this study we determine GW momentum flux from infrared limb emission measurements. The essential break-through of PREMIER compared with previous satellite measurements is to obtain 3D temperature distributions.

Gravity wave momentum flux is a higher-level data product, i.e. it is based on several processing steps in addition to measurement, calibration and retrieval. A full assessment of the quality of this data product therefore is based on an end-to-end simulation of the processing steps involved. In particular, it is necessary

- to retrieve 3D temperature distributions from the calibrated radiances
- to separate between the global scale background and the mesoscale GWs
- to characterize individual wave events in terms of amplitude, horizontal and vertical wavelength (i.e. in terms of the full 3D wave vector)

Given these steps are performed, one can calculate GW momentum flux according to

$$(F_{px}, F_{py}) = \frac{1}{2}\rho\frac{(k,l)}{m}\left(\frac{g}{N}\right)^2\left(\frac{\hat{T}}{\bar{T}}\right)^2 \tag{1}$$

where $(k, l, m) = (2\pi/\lambda_x, 2\pi/\lambda_y, 2\pi/\lambda_z)$ are the zonal, meridional and vertical wave number, g is the gravity acceleration, N is the buoyancy frequency, ρ is the density, $\bar{T}$ is the background temperature and $\hat{T}$ is the temperature amplitude.

All steps in this process are sources of error and should therefore be assessed both in common and separately. The principle overview of this end-to-end simulation is shown in Figure 1. In this end-to-end simulation the atmosphere is to be replaced by numerical models for which we know all atmospheric state variables (cf. task 2).

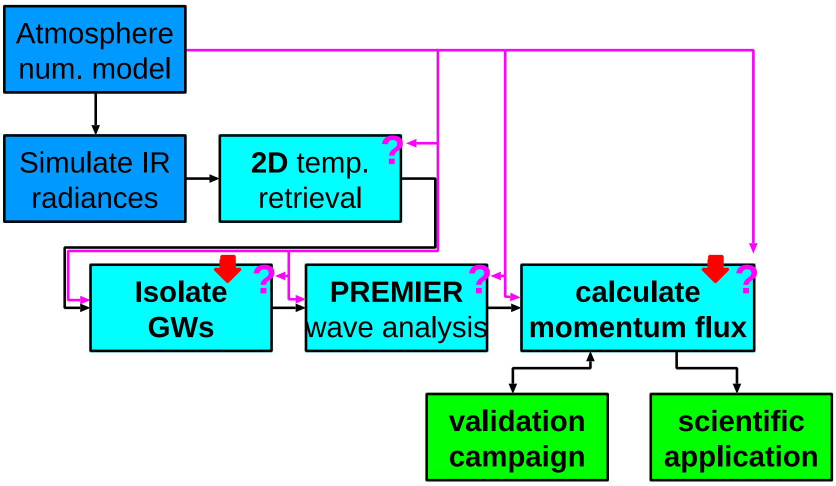

Figure 1: In the processing chain of this study we use temperatures of an atmospheric numerical model and simulate the PREMIER measurements. As we possess the full dynamical field and all dynamical variables, we know the “true” values for each processing step. By comparing (indicated by “?”) “true” values and processing results, the error of the single steps and the whole chain can be assessed.

3 Task 1: Literature study and definition of requirements

Gravity waves couple different layers of the atmosphere of waves by GW momentum flux. They also interact with other kind of atmospheric waves such as quasi-stationary planetary waves, Rossby waves, tides and quasi-two day waves. They may amplify, seed or damp these other kinds of waves and thus also indirectly influence atmospheric dynamics and chemistry. However, the main effect is the direct acceleration of the mean background flow. In generating GWs, momentum is transferred from the background to the waves and when the waves dissipate they transfer momentum to the background and thus accelerate or decelerate background winds (also called GW drag). As GWs often propagate several 10km in altitude, momentum can be transferred from the troposphere into the stratosphere, mesosphere and thermosphere by GW momentum flux. The most comprehensive way to study such coupling processes is the use of general circulation models (GCM). However, with few exceptions GCMs cannot resolve the relevant scales and dedicated submodels called GW parameterizations have to be used to describe the coupling processes. These are simplifications of our current knowledge on GWs.

Even more simplified, the momentum flux determines how much drag can be exerted, the phase speed and horizontal direction determines at which altitude the drag is exerted and the horizontal direction determines the direction of the drag. Thus, momentum flux, phase speed and direction are the chief parameters we need to determine. The accuracy shall be sufficient to solve questions relevant for e.g. climate modeling. However, what exactly are these open questions a) with respect to the GWs themselves and b) with respect to the impact of GWs on the whole atmosphere? Which information do we already possess, which can be gained by other instruments and which questions can PREMIER solve only? A comprehensive literature study was carried out covering the following themes

1. Open questions in GW theory, GW sources and the relevance/potential of different scales of GWs for conveying momentum flux
2. The role of GWs for climate models and numerical weather prediction
3. Use of data assimilation to gain information on GWs
4. Existing techniques on GW measurements

The literature study was carried out in 2009. For the final report new work in particular on the role of the stratosphere in general and of GWs in particular in climate research was incorporated. With respect to the four themes the following key-aspects were derived.

Open questions

Theory : The standard theory of GWs is based on the assumption that the variation of the background field is slow in comparison with the wavelength and wave period. This assumption is called the WKB assumption (for Wentzel-Kramers-Brillouin assumption). All GW parameterization schemes and also the deduction of momentum flux from PREMIER measurements are based on this assumption.

Q 1: What is the influence of WKB on measured GW momentum flux?
Q 2: What is the influence of WKB on GW parametrization schemes in e.g. climate models?

Gravity waves transfer momentum to the background wind when they break. The breaking process, however, is debated. In particular, do GWs remain at their saturation limit when they become instable or do they break down to a fraction of that amplitude? This shifts the interaction altitude and is therefore highly relevant for dynamical coupling.

Q 3: How does the breaking process shape the altitude profile of GW drag?

Case studies involving PREMIER measurements as well as measurements from complementary techniques for instance in a validation campaign could provide evidence needed to solve these questions. Some of the aspects of WKB theory are discussed in task 2 of this study.

Sources : Currently most Chemistry Climate Models employ two parameterizations for GWs, a parameterization for GWs excited by orography (mountain waves) and a parameterization subsuming all other sources called non-orographic GW parameterization. The latter is tuned in a way that the model reproduces the current state of the atmosphere and 1.) may compensate for other model deficiencies and 2.) cannot feedback changes of the GW-sources due to climate or weather changes in the model. For instance, if convection patterns change or the number of storms increase, the amount of generated GWs remains the same. These unspecific, tuned parameterization will, therefore, in future be replaced by parameterizations based on the physics of e.g. convection, fronts and jet-instability. Such physics-based schemes are nowadays still experimental, guided mainly by modeling (which does not converge with model-grid resolution) and has therefore a number of tunable parameters even for these physics-based parameterizations.

Q 4: How large is the GW momentum flux from different sources?
Q 5: What are the phase speed characteristics?

Different scales : Only waves which propagate from the troposphere into the stratosphere and mesosphere contribute to the coupling of these different compartments of the atmosphere. Gravity wave physics implies limits on the horizontal and vertical scales of the GWs which can propagate between these compartments and contribute to the coupling (e.g. *Preusse et al.*, 2008). We expect PREMIER to cover most of the essential part of the wave spectrum. This can be investigated with PREMIER data by comparing the measured distributions to the visibility limits of the instrument (cf. *Ern and Preusse* (2012)). Furthermore, the horizontal wavelength is important because it governs the lateral propagation.

Q 6: What are the prevalent horizontal scales?

The role of GWs for climate and weather

It has been long known that resolving the stratosphere in a global model requires taking into account the coupling by GWs. As currently weather and climate models extend their upper lids at least to stratopause altitudes the need for an improved representation of GWs is evident. Processes majorly influenced by GWs are summarized in Figure 2. Processes which are driven chiefly by GWs are shown in red. It is evident that GWs play an important role in shaping the middle atmosphere. The shown middle-atmosphere processes in turn influence surface climate and weather. For details see the final report and literature therein.

These links are known in principle, but are lacking quantification:

Q 7: How large is the relative contribution of GWs compared to other wave types in driving middle atmosphere circulation?
Q 8: What are the sources of these GWs?
Q 9: How will the GWs and the driving change in future?

Future changes (Q9) can of course neither be measured nor extrapolated from measurements. However, using physics-based schemes a sound prediction will become possible. In addition, with a multi-year record some separation in source changes and wind modulation will become possible, i.e. we will be able to discern to which extent long-term variations are due to altered sources and to which extent they are caused by wind filtering occuring between source and observation altitude.

Role of data assimilation

Data assimilation has been used to infer the non-resolved drag in a GCM. The general principle is as follows. The assimilation of observations adjusts the GCM to the real state of the atmosphere. One then compares the drag required for the "observed" dynamical evolution of the system with the drag provided by the processes resolved by the model. The difference is attributed to momentum deposition by GWs (*Pulido and Thuburn*, 2005, 2006). Assimilation may also be used to combine different measurement techniques in a synergetic

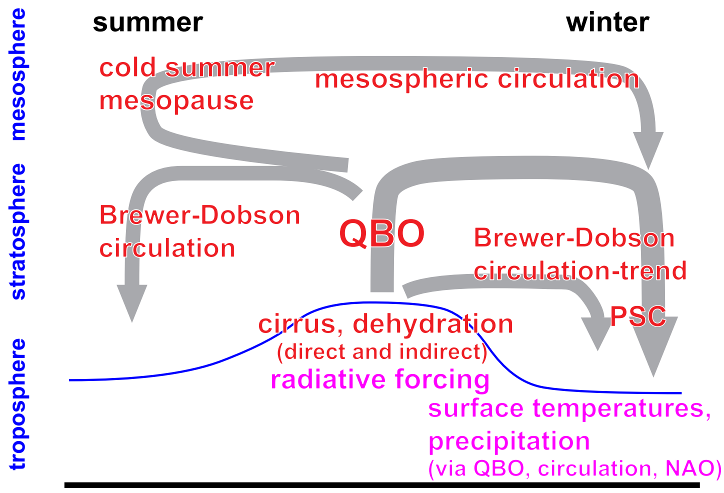

Figure 2: Schematic sketch showing the different compartments of the Earth's atmosphere, the tropopause (blue line) and the general mean circulation (fat gray arrows, Brewer-Dobson circulation in the stratosphere). Processes where GWs have major direct impact (order of 50%; larger in the mesosphere) are given in red. Indirect effects of e.g. circulation changes are denoted in pink.

evaluation, and facilitate comparisons for larger miss-distances and miss-times between observing platforms. Finally, assimilation of e.g. GW momentum flux into the GW parameterization scheme of a prediction system might enhance its predictive skill. The latter two applications are unprecedented. Some aspects of the use of data assimilation in a validation campaign are investigated in task 8.

Existing measurement techniques

We postpone the discussion of existing techniques to task 8 where developments in the last two years are also reflected.

3.1 Requirements

From the processes of atmospheric dynamics majorly affected by GWs and the scientific questions in the fields we can deduce requirements for substantial scientific progress. For a better overview we first repeat the questions:

Q 1: What is the influence of WKB on measured GW momentum flux?
Q 2: What is the influence of WKB on GW parametrization schemes in e.g. climate models?
Q 3: How does the breaking process shape the altitude profile of GW drag?
Q 4: How large is the GW momentum flux from different sources?
Q 5: What are the phase speed characteristics?
Q 6: What are the prevalent horizontal scales?
Q 7: How large is the relative contribution of GWs compared to other wave types in driving middle atmosphere circulation?
Q 8: What are the sources of these GWs?
Q 9: How will the GWs and the driving change in future?

Note that *Q 4* and *Q 7* both consider the same topic, GW sources, but one from the perspective of the source processes and one from the perspective of the global momentum balance.

Global measurements

The processes highlighted in Figure 2 are driven by the global momentum and energy balance. In order to investigate such momentum balances we need to determine the zonal mean of the zonal component (i.e. west-east component) of the momentum flux. As this averages over positive (eastward waves) as well as negative (westward waves) values we emphasize this fact by calling this quantity zonal mean net pseudomomentum flux in zonal (or x) direction (NX-GWMF). This quantity can be only calculated from global measurements.

Global measurements are required for *Q 4*, *Q 6*, *Q 7* and *Q 8*. Dissipation of GWs (*Q 3*) may be studied from case studies, but requires confinement by measurements on the global scale, too.

Altitude range

Gravity wave drag is given by the vertical gradient of NX-GWMF. Measurements therefore should cover the entire stratosphere. Also, the vertical spectrum of GWs changes with altitude. Does also the horizontal spectrum change?

Measurements covering the whole altitude-range of the stratosphere are required for *Q 3*, *Q 4*, *Q 6*, *Q 7* and *Q 8*.

Accuracy of NX-GWMF

Current satellites can not infer the direction of the waves and only absolute values of GWMF can be inferred. First attempts are made to use these global climatologies for guiding GW parameterizations in GCMs, for instance, by the aforementioned ISSI team. Comparisons of the vertical gradient of absolute value of GWMF between 25 km and 40 km altitude currently differ by a factor of 6 for the estimates from satellites and GCM, but are still inconclusive because of the large error ranges of the satellite estimates. In addition, in order to confine also the impact on the background wind (i.e. the tendencies due to the GWs) the direction of the waves is required. Estimates of NX-GWMF with errors of the order of 30 % could provide true guidance for GW parameterizations. Comparing NX-GWMF below and above strong changes of the wind or buoyancy frequency (potential WKB violation) can clarify the importance of partial reflection[1].

The accuracy requirement is needed for *Q 2*, *Q 3*, *Q 4*, *Q 6*, *Q 7* and *Q 8*.

In addition to zonal mean values we need also to characterize single GW events in case studies. For instance, one could consider mountain wave events at Scandinavia employing PREMIER, additional techniques and different models. These can be compared at different altitudes in order to answer *Q 1* and *Q 2*.

Spectral Characterization

The altitude where a GW interacts with the background wind is in the first instance determined by its horizontal phase speed and propagation direction. The measurements should therefore allow to infer spectral characteristics as well as direction for guidance of physics-based source parameterizations.

The requirement is needed for *Q 2*, *Q 4*, *Q 5*, *Q 6* and, indirectly, *Q 8*.

[1]Partial reflection occurs when a wave encounters a dispersive medium. The best known example is light at a water or glass surface: a large part of the light is transmitted into the medium and a smaller part is reflected. A GW reacts similarly to an abrupt change in buoyancy frequency or horizontal winds, cf. e.g. *Kim et al.* (2012). The wave will continue propagating upward, carrying the larger part of the GWMF it has below the reflection layer, but will also generate a reflected downward propagating wave.

Summary

In summary, we need to determine the momentum flux, direction and phase speed of individual wave events, classify these for different source types and we need to determine zonal mean zonal net momentum flux NX-GWMF at an accuracy of the order of 30 % or better.

4 Task 2: Atmospheric numerical modeling

Atmospheric models are the basis of this study. It is in the nature of GWs and part of the particular importance of the PREMIER mission that a global model resolving GW excitation and dissipation without the use of parameterizations is many orders of magnitude too computationally expensive. The models employed, therefore, have a limited representation of reality.

This, however, only moderately affects the aims of this study. The only strict request we have is that the different state variables, i.e. model temperatures and winds are consistent, because the basis of the assessment is to compare GWMF deduced from sampled and/or processed PREMIER temperatures with GWMF directly calculated from the model winds taken as the reference. Unrealistic amplitudes or wavelengths will cancel out at first order and only residuals from other processes may enter the error assessment (e.g. too low GW amplitudes may give an overestimate of the relative importance of planetary waves in the removal of the background). The models therefore need to be realistic only to a certain extent. Because their fidelity cannot be ascertained from first principles, in this study we use only selected models which were compared to observations, mostly in published studies.

Tests of the full observational filter, the detrending (separation of global and mesoscale waves) and the wave analysis need to be performed and the model data have to be selected accordingly. In addition, we need model data for the test of the WKB assumption in the polarization relation. This cannot be achieved with a single model. In general, the finer the model grid resolution the smaller the domain of a model. In addition, the effective resolution of a model is about 6-10 model grid points. Therefore, we have selected a variety of models to cover all aspects of this study; an overview is given in table 1.

Table 1: Requirements for testing the individual steps of the processing chains and modeling runs matching them. The first column lists the requirements, the rows show the different topics to be investigated. We fill only the Matrix elements where a requirement is made for a scientific topic and there give the models matching this requirement.

requirement	2D retrieval	GW isolation	GW analysis	momentum flux
fine model grid (5-10 km)	York, CPI, UNN, CoRA			
domain extends >2000 km	York, Yonsei, CPI, UNN, ECMWF			
model top >60 km	Yonsei, CPI, ECMWF			
consistent ozone	ECMWF			
global data		ECMWF		
realistic GWs, PWs		ECMWF		
GWs up to 40 km			Yonsei, CPI, ECMWF	
different sources			Yonsei, CPI, ECMWF, York	
temp. and wind			all	all
WKB not used				all
Space-time spectra				Yonsei

5 Task 3: Retrieval

Task-3 of the ESA gravity wave study deals with the retrieval of stratospheric temperature data from simulated radiance measurements of the proposed PREMIER Infrared Limb Sounder. The task is divided into four work packages: (1) selection of a priori data, (2) selection of micro windows, (3) development of forward model and retrieval algorithms, and (4) analysis of retrieval errors and characteristics.

Within the optimal estimation retrieval approach applied in this study, the retrieval result is obtained as a combination of true data (i. e. scenario data provided by Task-2) and a priori data. The a priori data should describe as well as possible the knowledge about the atmospheric state before a measurement is made. It provides regularization in case the inverse problem is under- or over-determined. In particular, a priori data on the mean atmospheric state at different altitudes, latitudes, and seasons of the year are required. Corresponding standard deviations capturing the variability of atmospheric temperature are needed as well. A reference database was created for the project. The database contains profiles of temperature, pressure and thirty-six trace species (i.e. infrared-active minor constituents of the atmosphere). In addition to the RAMstan climatology, a multi-year dataset of ECMWF operational analyses was used to estimate temperature covariances with respect to the vertical, longitudinal, and latitudinal direction. The ECMWF covariances were used as a guideline to tune the first-order autoregressive model which is used in the tomographic retrieval system to model the a priori temperature covariances.

Optimal spectral windows have been selected in order to minimize the retrieval errors due to noise and forward model parameter errors, e. g. uncertainties of interfering species. For this study the microwindow selection has been significantly enhanced. Four sets of microwindows were selected for different combinations of two detector configurations and two retrieval ranges: stratosphere only, or full range covering both troposphere and stratosphere. For the stratospheric retrievals, pressure and temperature are retrieved jointly with ozone. For the full-range retrievals, it is also necessary to retrieve water vapor. A linear error analysis is applied first to a 'perfect instrument', i.e., one which is assumed to be perfectly characterized, with NESR the only instrument contribution to the retrieval error. The other contributions, the 'atmospheric errors', arise from 1σ climatological uncertainties in interfering species, i.e., molecules other than those retrieved. The CO_2 uncertainty is included as an error. Errors due to ignoring non-LTE effects are also included. The linear error analysis considering just the atmospheric errors and noise meets the target requirement for 1-D retrievals. In addition, a variety of different instrument characterization errors were tested. It was found that vertically uncorrelated gain and pointing errors may have significant impact on the retrieval error budget, but could be mitigated.

A fast and accurate radiative transfer model is essential to solve large inverse problems in atmospheric remote sensing. We adapted the Juelich Rapid Spectral Simulation Code (JURASSIC) for the tomographic temperature retrievals. JURASSIC was previously used for forward model and retrieval studies for several satellite- and air-borne remote sensing experiments. A major feature of JURASSIC is the use of the emissivity growth approximation (EGA) to accelerate radiative transfer calculations. Compared with conventional line-by-line calculations the EGA approach is several orders of magnitude faster. A detailed comparison of JURASSIC with the line-by-line model KOPRA was carried out in this study to assess the accuracy of the fast model. During the course of the study the instrument model was extended in order to assess retrieval errors due to pointing, radiometric offset and gain, as well as spectral shift and resolution.

The retrieval of atmospheric data is based on the optimal estimation approach. The 'optimal estimate' of the atmospheric state is found by minimizing the deviations between forward model simulations based on the current estimate of the state and the actual radiance measurements, as well as minimizing the deviations between the estimate and the a priori. Deviations are normalized by the measurement error covariance and the a priori covariance, respectively. Since the retrieval problem is moderately non-linear the Levenberg-Marquardt method is used to find the minimum of the cost function iteratively. A multi-target approach is applied, i. e. all retrieval targets can be derived simultaneously and correlations between the different quantities are fully taken into account. The retrieval processor provides a detailed error budget for the 2-D retrievals as well as retrieval characteristics in terms of averaging kernel matrices. For this study we also derived the observational filter from the averaging kernel matrix. The observational filter is of particular interest for gravity wave studies because it describes the retrieval response to temperature wave perturbations with different vertical and horizontal wavelengths (e.g. *Preusse et al.*, 2002). The observational filter for one of the retrieval data sets produced in the study is shown in Fig. 3.

In total, four retrieval data sets were produced during the course of the study. The error budget and characteristics were analyzed for each data set. The first data set is obtained by a linear mapping approach, based on given averaging kernels and retrieval noise levels obtained from 2-D non-linear retrieval simulations. A first version used simplified error assumptions, the version we consider in more depth is called Linear Retrieval V2. The other three data sets are based on a non-linear retrieval approach and represent different levels of complexity in terms of state vector and measurement vector configurations. A version with one single micro-window (MW) is referred to as Non-Linear Retrieval V1, a version with 5 MWs is referred to as Non-Linear Retrieval V2.

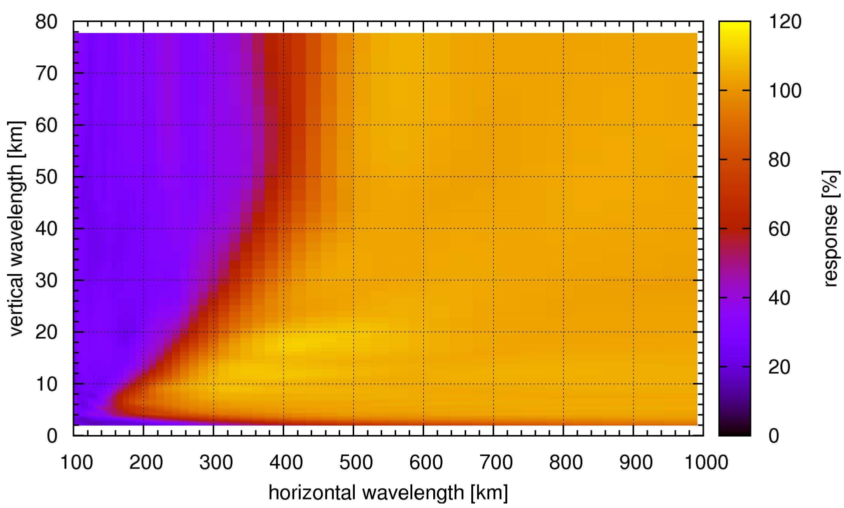

Figure 3: Observational filter for a full 2-D non-linear retrieval. Color coding indicates the maximum retrieval response to plane wave perturbations in the temperature field. The horizontal wavelength refers to the projection of the wave in the x-z plane which is relevant for the sensitivity of the 2D retrieval; in general, the wavelength of the 3D GW is shorter.

6 Task4: Separation of GWs and planetary scale background

Any measurement, for instance a vertical profile of temperature, contains structures due to a variety of processes including the zonal mean structure, Rossby waves, tides and various other types of planetary scale waves and gravity waves. In order to analyze the PREMIER measurements for GWs therefore the first step needed is to separate the planetary scale structures from the mesoscale signatures. Also we have to assume that these mesoscale structures are chiefly due to GWs. This is an assumption and will be justified by the assessment, task 6.

Traditionally (e.g. *Fetzer and Gille*, 1994), an estimate of waves with zonal wavenumber 0 (zonal mean) to 6 is performed and subtracted from the measurements. This approach is feasible because:

- Planetary scale waves have their maximum at zonal wavenumbers 1 and 2 and spectral power decreases rapidly for higher wavenumbers. This causes a spectral gap between the planetary waves and the GWs. Note that this applies in the middle atmosphere but not necessarily below the tropopause.
- Unlike trace species, temperature structures are dissipated by both turbulent and radiative damping. While there are many long-lived filaments in tracers, the remnants from instable planetary waves decay rapidly.
- Momentum flux is inversely proportional to the horizontal wavelength. Potential remnants from PWs not fully removed in the subtraction of the background atmosphere will have long horizontal wavelengths and, accordingly, low momentum flux.

Technical approach

The method chosen is to interpolate the temperature data in the vertical and along track onto a grid of e.g. 1km altitude and 0.5 degree latitude. For each latitude a sinusoidal fit of the shape

$$T_i = \sum_k A_k \sin(k\phi_i) + B_k \cos(k\phi_i) \tag{2}$$

is performed, with T_i the individual temperature measurements at associated longitudes ϕ_i, k the zonal wavenumber and A_k and B_k the respective amplitudes.

At a single day there are 15 orbits, each with an ascending and a descending orbit leg and for each of the orbit legs 12 tracks associated with the individual spatial-sample columns in the PREMIER images, that is 360 data points. However, GW structures may be coherent in the 12 tracks and therefore map into the wave 0-6 planetary wave estimates. These GW structures form super-imposed short-scale perturbations on the broader PW scale features. By polynomial-fit smoothing of the amplitudes A_k and B_k over altitude and latitude, the background estimate is improved. For the smoothing a 4^{th} order polynomial in the vertical and a 3^{rd} order polynomial in the horizontal is used.

Technical assessment and optimization of smoothing parameters

The method is tested for sampled ECMWF data. Validation/assessment encompasses two aspects: First, the quality of the separation into global and mesoscale structures and second the question whether the remaining structures are really GWs. The first question is technical and can be assessed within this task. The second question may be answered via tasks 6 and 7, i.e. whether the isolated mesoscale temperature structures have the properties of GWs and match the momentum flux from the model winds.

For regularly gridded, synoptic data, the Fourier transform projects the variances onto an orthonormal basis of waves and so solutions for waves 0-6 are unique and error-free. The assessment is performed by comparing sampled temperatures detrended by the planetary wave estimate $T_{\delta PW6}$ (the detrending result) with data which are first detrended by a Fourier transform and afterwards sampled to the measurement locations T_{FT6} (the "truth"). We now calculate altitude profiles of the global standard deviations $\sigma(T_{\delta PW6})$, $\sigma(T_{FT6})$ and $\sigma(T_{\delta PW6} - T_{FT6})$ (result-"truth"). A good detrending is characterized by a value of $\sigma(T_{\delta PW6} - T_{FT6})$ small in comparison to the true GW standard deviation $\sigma(T_{FT6})$ and an estimated $\sigma(T_{\delta PW6})$ which is close to $\sigma(T_{FT6})$.

We find that

- combination of ascending and descending orbit legs in a common fit (ADC) largely improves the results with respect to using separate fits for ascending and descending orbit legs (ADS)
- polynomial smoothing over 12-15° latitude and 5km in the vertical is optimum for ECMWF data. The smoothing parameters for the various seasons are largely consistent.
- The quality of the results depends strongly on the swath width. A 200 km swath width (threshold of the PREMIER requirements) induces a substantial performance loss.
- Using a 360 km swath, a common fit for ascending and descending orbit legs and optimum smoothing parameters, $\sigma^2(T_{\delta PW6} - T_{FT6})$ is about 20 % of $\sigma^2(T_{FT6})$ and $\sigma^2(T_{\delta PW6})$ underestimates $\sigma^2(T_{FT6})$ by about 10-15 %.

The underestimation of $\sigma^2(T_{\delta PW6})$ in comparison to the true value $\sigma^2(T_{FT6})$ is caused by erroneously attributing GW structures to PWs and thus lessening the GW amplitudes. It should be noted that these effects are more likely to occur for GWs with wave fronts in the east-west direction (i.e. with preferential meridional propagation direction). In addition, larger wavelength waves are stronger affected and the loss in momentum flux is therefore smaller than that in variance (cf. task 6).

7 Task 4: GW analysis tool

The back-bone of the whole study is the GW analysis tool. Gravity waves in the middle atmosphere have typical horizontal wavelengths from several 10 km to several 100 km. Wavelengths of e.g. 500 km are quite typical. This is long compared to the swathwidth and a standard Fourier transform cannot be applied. In addition, the vertical extent of the fitting window should be kept small as

1. GW vertical wavelengths change with altitude according to the vertical gradient of the horizontal wind,
2. GW amplitudes are expected to change due to momentum conservation in conservative propagation (exponential amplitude growth) and due to dissipation (amplitude decay) e.g. close to critical levels, and
3. vertical gradients and thus acceleration can only be localized if a) a sufficient number of independent values exists and b) the values can be attributed to reasonably localized altitudes.

We therefore want to restrict the vertical extent of the analysis volume to 10 km. Still, in the stratosphere vertical wavelengths of 10 km and longer are common.

A wave analysis is chosen which determines a few (e.g. 2) leading wave components from a given analysis volume. Still we require that in a statistical ensemble the spectral properties are captured. Summarizing the requirements the wave analysis shall

- provide the full wave vector and amplitude of the two leading wave components in a local analysis volume
- have a vertical extent of the analysis volume that does not exceed 10 km
- be capable of analyzing waves which have larger wavelengths than the size of the analysis volume
- cope well with strong intermittency, i.e. strong variations of wave parameters on comparable short spatial scales
- capture in a statistical ensemble the spectral properties

7.1 Methods tested

Vertical MEM/HA and horizontal phase gradient method

Current estimates of momentum flux from satellites are based on combining a sliding wave analysis on single vertical profiles based on the maximum entropy method (MEM) and sinusoidal fits (harmonic analysis; HA, cf. *Preusse et al.* (2002)) with a phase-difference analysis between the profiles (e.g. *Ern et al.*, 2004; *Alexander et al.*, 2008; *Ern et al.*, 2011). This method can also cope with the poor horizontal sampling of current-days satellites. When applied to high-quality PREMIER data we find that the method produces phase and hence wave-direction inversions. These can be corrected but only at the price of information loss. Noise will affect the single profile analyses and lead to much larger scatter in the results than a common evaluation of all input data. Conclusion: While the method is very robust for poor data it cannot reach the ambitious aims we have for the PREMIER mission.

Wavelet analysis

Wavelet analysis is especially developed for the spectral analysis of data with non-stationary amplitudes and should therefore be particularly suited for GW analysis. For this study a tool for 2D wavelet analysis was developed. A suitable wavelet form was selected. Test analyses were made with idealized data and one real orbit segment.

The tests showed that in a localized volume the method was not always able to correctly recover both amplitudes of a superposition of two waves. The method proved to be computationally too expensive to be applied on several weeks of PREMIER data.

Sinusoidal fit of distinct waves in a 3D data cube (S3D)

We therefore decided on a relatively simple method. The Premier data are first subdivided into relatively small analysis volumes of e.g. 360 km x 350 km x 10 km across-track, along-track and in the vertical. For each volume subsequent least-square fits are performed. For each wave component j the algorithm minimizes the squared deviations

$$\chi^2 = \sum_i \frac{(Y_i - f(X_i))^2}{\sigma_i^2} \tag{3}$$

of the function

$$f(X_i) = A_j \sin(k_j x_i + l_j y_i + m_j z_i) + B_j \cos(k_j x_i + l_j y_i + m_j z_i) \tag{4}$$

where (k_j, l_j, m_j) is the wave vector for the j^{th} wave component and A_j and B_j are the respective amplitudes. Y_i are the individual measurements for the locations $X_i = (x_i, y_i, z_i)$ and are in our case the temperature residuals, that is T'. As for a given wave vector the least-square problem in A_j and B_j can be solved arithmetically, a variational method to minimize χ^2 is required only for the wave vector. At the moment nested intervals and an initial wave vector provided from 3D Fourier transform (maximum amplitude of the FT) is used. After determining the optimal solution for wave component j this is subtracted from the temperature fluctuations and the least-square fit for component $j + 1$ is performed. Note that in this way for each wave component the solution selected is the one which describes most of the remaining variance (it is not the solution with the largest amplitude).
Note also that waves with wavelengths longer than the extent of the fitting cube have wavenumbers between zero (constant component) and the smallest wavenumber in the respective direction. They can hence be captured by subdividing a 'natural' grid from a Fourier transform by finer intervals. A wavelength smaller than the Nyquist limit, however, is of course aliased into the resolved spectral region as by any other spectral estimation method.
For brevity, in the discussion below we will call this approach of sinusoidal fits in 3D data cubes below "few-wave decomposition" or "S3D method".

Validation of the S3D method

The S3D method is simple, but lacks theoretical background. For instance the method does not fulfill the Parseval theorem. Also fitting wavelengths larger than the analysis volume appears questionable. Therefore extensive validation was required.

We have first tested the method using idealized data and recovering a superposition of two given sinusoids with different wavelengths and amplitudes. The method was always able to recover both wavelengths with good accuracy even if the wavelengths exceeded in two dimensions the size of the analysis interval.

We then tested the method against space-time Fourier transform for a case study of typhoon modeling. The results were published by *Lehmann et al.* (2012). A typhoon is a particularly interesting test case: the convection in the typhoon generates a wide spectrum of GWs with phase speeds ranging from 0 to more than 50 ms^{-1} (and, accordingly, vertical wavelength frequently exceed 10 km) and a wide range of horizontal wavelengths, the sources are located in the typhoon center and the spiral bands and the wave characteristics are very different upstream and downstream of the source. Thus, there are both rich spectra and high spatial variations.

The results are very encouraging. Vertical profiles of positive and negative momentum fluxes and of net momentum fluxes from FT and S3D agree within 10 % or better. The main spectral features are recovered, as Figure 4 shows.

8 Task 5

The setup of the ray-tracing tool is described together with the results in task 7.

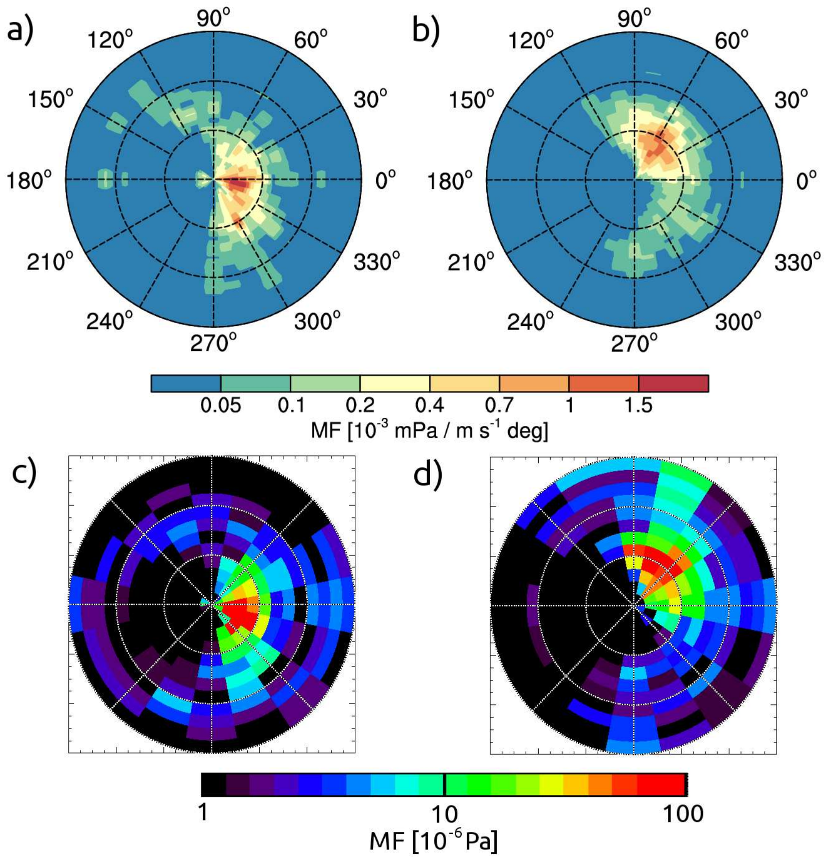

Figure 4: Momentum flux spectra in terms of phase speed and propagation direction calculated via (upper row) Fourier transform and (lower row) S3D for (left column) 7 July, 01 UTC to 8 July, 06 UTC and (right column) 9 July, 13 UTC to 10 July, 18 UTC at 25 km altitude. Please note the logarithmic color scale for the S3D results. Circles indicate 20 ms^{-1} phase speed, maximum shown phase speeds are 60 ms^{-1}. Adapted (combined) from Figures 4 and 6 of *Lehmann et al.* (2012).

9 Task 6: Momentum flux assessment

Reference data for assessment

For the quantitative assessment of momentum flux it is important to be precise on quantities and approximations. The acceleration which enters the equation of motion formulated for fixed coordinates on a rotating sphere is the vertical flux of horizontal pseudomomentum (see discussion in the theory-chapter of the final report). The basic definition is in terms of the wind residuals u' and w'

$$F_p x = \bar{\rho}(1 - \frac{f^2}{\hat{\omega}^2})\overline{u'w'} \tag{5}$$

where $\hat{\omega}$ is the intrinsic frequency and f is the Coriolis parameter. For this $\hat{\omega}$ has to be known which involves a wave analysis and thus would induce error into the reference. We rather will divide the temperature based GWMF by the factor $(1 - f^2/\hat{\omega}^2)$ which allows us to calculate a true reference from the full, unsampled ECMWF data (cf. discussions in the final

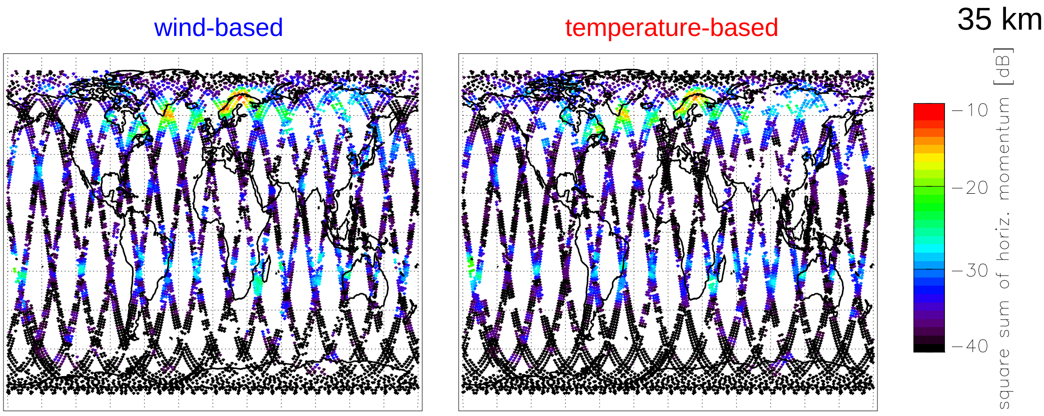

Figure 5: Global maps of absolute values of mid-frequency-approximation pseudomomentum flux from (left) winds and (right) temperatures at 35 km altitude and for 29 January 2008.

report), which is not affected by sampling issues and errors due to a wave analysis. Note that GW parameterizations usually use the assumption that the wave frequency is substantially larger than the Coriolis parameter and smaller than the buoyancy frequency $f \ll \hat{\omega} \ll N$ (mid-frequency approximation) and neglect accordingly the factor $(1 - f^2/\hat{\omega}^2)$. For comparison of single wave events we refer to wave analysis of winds sampled to the measurement (respectively retrieval grid) locations. In this way issues of sampling do not affect the comparison of the individual waves.

Comparison of maps

Figure 5 compares the absolute value F_a of mid-frequency pseudomomentum flux[2] from temperatures with the same quantity deduced from model winds, with F_a being defined as

$$F_a = \sqrt{\sum_j \tilde{F}^2_{px,j} + \tilde{F}^2_{py,j}} \tag{6}$$

where the sum runs over the spectral components fitted for each analysis cube[3]. We find good correspondence in the absolute values, the general structures and also a point-to-point correspondence of single events.

In order to quantify the level of agreement we compare the two data sets point-by-point by means of statistical analysis and calculate the correlation coefficient, the slope via Least Square Fit and a linear Least Absolute Deviation (LAD) fit. The data are, in general, well aligned along these fit lines but show some scatter. The width of the distribution of this scatter perpendicular to the fit line is used to characterize the individual-location error. The correlation coefficient measures whether the relative structures correspond, the slope gives the sensitivity in particular for the larger GWMF values, the linear constant of the LAD fit the sensitivity in particular for the smaller GWMF values. For a systematic overview we calculate these quantities for all 35 days and give the average in table 2.

[2]That is, the intrinsic frequency $\hat{\omega}$ of the wave is large compared to the Coriolis parameter f and small compared to N. In particular it means that the correction factor $(1 - \frac{f^2}{\hat{\omega}^2})$ in (5) is neglected.

[3]Note that the definition of the absolute momentum flux is somewhat arbitrary. In using the square sum (RSS) of the two wave components in each cube one emphasizes the stronger events somewhat, more compatible with results from current sensors.

Zonal mean net zonal momentum flux

An example for NX-GWMF in mid-frequency approximation from temperatures, sampled winds and full model winds is shown in Figure 6. The bars indicate the statistical errors of the mean values for the sampled data and therefore express the influence of the natural variability. In the example shown, all features well match inside the natural variability.

Also for the NX-GWMF we want to gain a statistical overview. The first measure we use is the relative size of the latitude-sum absolute deviations:

$$\delta_{LS} := \frac{(\sum |F_q - F_r|)}{(\sum |F_r|)} \tag{7}$$

where F_r denotes the reference data set, F_q the investigated data set, || absolute values and the sum $\sum$ runs over the individual latitude bins.

The second measure is based on the fact that in the summer hemisphere waves originate from subtropical convection and have predominately eastward net flux and in the winter hemisphere waves are associated with the polar night jet and have predominantly westward net flux. If we integrate over these respective hemispheres, we integrate, basically, over these two features and hence the relative deviations of the hemisphere average are meaningful. Comparing to the sampled-wind averages the sampling of the global distribution due to the limited swath-width cancels because it is inherent in both data sets. Comparison to the full data shows this additional effect in combination with a different vertical smoothing: The fits are performed in an analysis volume of 10 km vertical extent. The reference values are cal-

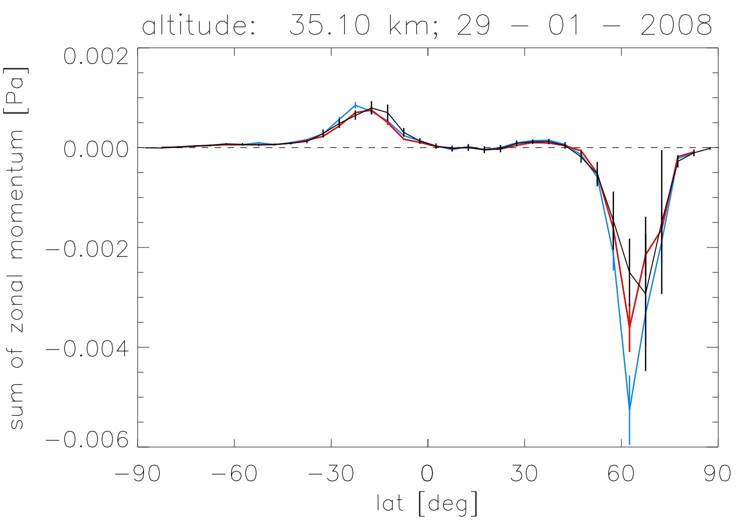

Figure 6: Zonal mean net zonal pseudomomentum flux NX-GWMF in mid frequency approximation for 29 January 2008 and 35 km altitude. The red line shows values deduced from temperatures, the blue line shows values deduced from wind data sampled to the PREMIER locations and the black line shows the momentum flux directly from the ECMWF winds. Vertical bars give the statistical errors of the mean values for the red and blue curve. The GWMF from ECMWF is averaged over 5 degree latitude and 10 km altitude in order to be compatible with the values from the S3D analysis and the error bars indicate the standard deviation inside these averaging boxes.

culated for each individual altitude. In order to make these values comparable the reference values are smoothed by a 10 km vertical boxcar function.

Due to the large intermittency and the compensation of positive and negative fluxes, NX-GWMF is subject to larger errors. In particular for the hemispheric fluxes one needs to calculate one week averages for a good correspondence, though daily averages are still capable of capturing large day-to-day variations of up to a factor 3 in the hemispheric fluxes. For the assessment of hemispheric NX-GWMF we use only months where NX-GWMF is clearly distinct from zero (either due to the winter polar vortex or summer-time convection) that is January, July and August for the Northern Hemisphere (NH) and January, July, August and September for the Southern Hemisphere (SH). Again, relative deviations are given in table 2.

The following “retrieval” cases described in section 5 are assessed:

- Sampled data (no retrievals)
- Linear Retrieval V2
- Non-linear Retrieval V1
- Non-linear Retrieval V2

In principle these retrievals can be combined with three different methods of detrending: interpolation of the Fourier-transform on the full data set to the retrieval grid position as well as ADS (separate detretending for ascending and descending orbit legs; cf. 6 and detrending section in the final report) and ADC (common detrending) removal of planetary waves. We will show here a selection of cases (note that each product assessed here requires a full processing!).

Discussion of the assessment

Sampled, Fourier detrended data show, dependent on altitude, a low bias of the temperature-based momentum flux values. We surmise that this is, at least to some extent, an effect of the ECMWF data, previous investigations and the method validation giving evidence of this. We find that the detrending adds a 5-10 % low bias, consistent with the discussion above. Retrieved, detrended data are low biased up to 30 % - an exception are the values at 45 km altitude which is likely an effect of the retrieval upper boundary causing artificial structures.

On close inspection we found that the chosen acceleration method for the retrievals to process 2000 km along-track slices with a constant kernel matrix caused edge effects. These spurious waves significantly lower the performance estimate shown in the table and hence we recommend further work on the retrieval processor, if PREMIER is selected for the mission after phase A.

Table 2: Overview over the assessment parameters from the individual processing steps. The first columns specifies the generation of the temperature data set, the second the method of the separation between mesoscale GW and planetary scale background. The slope from the correlation analysis represents the sensitivity (i.e. 1 minus the slope is the accuracy or systematic error) the relative width gives the precision for single wave events. The zonal mean (ZM) values characterize zonal mean net zonal pseudomomentum fluxes. The average of the relative deviation at individual latitudes indicates the reproduction of the latitudinal structure, the relative deviations of the total hemispheric flux for the NH and SH are given with respect to sampled winds (S) as well as the true reference of the full ECMWF data (R).

temperatures	detr.	altitude [km]	corr. coeff.	slope	relat. width [%]	ZM rel. dev. [%]	ZM NH S [%]	ZM SH S [%]	ZM NH R [%]	ZM SH R [%]
sampled	FT	25	0.88	0.82	24	25	9	10	18	22
sampled	ADC	25	0.87	0.76	24	30	26	20	33	31
sampled	ADS	25	0.86	0.72	25	33	33	26	39	35
linear V2	ADC	25	0.85	0.70	26	34	27	20	34	31
linear V2	ADS	25	0.84	0.67	24	37	35	27	41	37
non-lin. V1	ADC	25	0.84	0.82	30	35	19	16	28	33
non-lin. V2	ADC	25	0.76	0.77	40	35	23	12	38	30
sampled	FT	35	0.91	0.78	21	21	15	14	15	20
sampled	ADC	35	0.90	0.71	21	29	29	23	30	30
sampled	ADS	35	0.89	0.67	23	34	36	26	37	32
linear V2	ADC	35	0.90	0.64	21	31	30	27	32	34
linear V2	ADS	35	0.89	0.61	21	38	39	32	41	39
non-lin. V1	ADC	35	0.82	0.71	25	26	24	20	24	24
non-lin. V2	ADC	35	0.87	0.77	27	25	23	14	32	32
sampled	FT	45	0.90	0.90	22	18	11	9	11	11
sampled	ADC	45	0.88	0.80	23	25	22	18	25	20
sampled	ADS	45	0.86	0.75	25	30	30	25	33	25
linear V2	ADC	45	0.88	0.70	21	30	24	22	33	28
linear V2	ADS	45	0.87	0.64	22	37	32	27	41	34
non-lin. V1	ADC	45	0.86	0.61	24	37	31	32	40	40
non-lin. V2	ADC	45	0.85	0.67	26	33	27	22	45	44

10 Task 7: Scientific demonstration by backward ray tracing

Ray tracing considers a wave packet of a distinct wave with given wave parameters and calculates it way through the atmosphere based on its group velocity. The horizontal group velocity is, in general, of the same magnitude as the background wind, the vertical group velocity in the magnitude range of 0.1 km/h to 10 km/h. Gravity waves hence propagate upward on oblique ray-paths sometimes staying close to their source, sometimes drifting with the wind for thousands of km.

Ray tracing can only be applied if the background wind is known (which is given by weather center data assimilation systems like that at ECMWF) and if the wave is fully characterized, e.g. in terms of its full 3D wave vector. Therefore ray-tracing is possible for PREMIER but not for current-day satellites.

One example for backward ray-tracing is shown on the title page of this report. Starting from the centers of the S3D analysis cubes rays trace the propagation path backward to the southern tip of Greenland, indicating that the waves in the example are mountain waves.

A second example is the global distribution shown in Figure 7. Shown are the PREMIER measurement tracks (white dashes) where the rays are initialized and the end points of the rays. Color code gives altitude. In wide regions of the globe the waves can be backtraced almost to the ground (indicated by blue color). This does not mean that the source is necessarily in the troposphere; the source can be at any altitude above this lowest altitude. In other regions a predominance of red or yellow colors indicate that the waves cannot be traced further down than to the lowermost stratosphere or the tropopause region.

We have indicated some regions of special interest by pink colors. First we find a cluster of ray-origins (i.e. ends of the back-trajectories) west of Norway over the Norwegian Sea. By

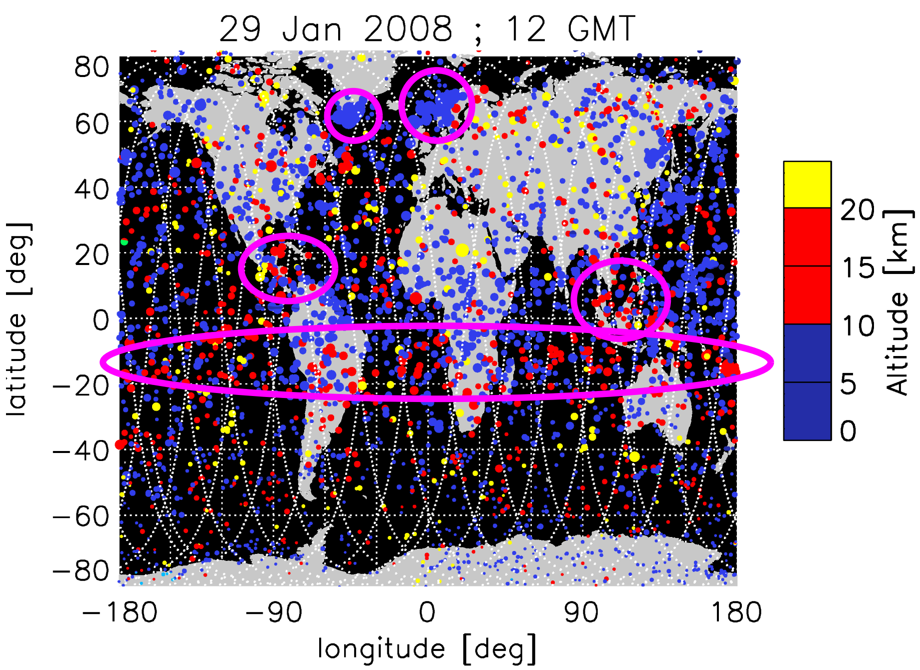

Figure 7: World map of back traces from 25 km altitude for 29 Jan. 2008. Shown are the end points of the rays. The size of the dots is scaled with the observed GW temperature amplitude.

inspection of the wind data we found that these correspond to a low pressure system with very high wind velocities in the troposphere (e.g. 500 hPa). A second cluster of waves marks the mountain waves from Greenland shown in the 3D illustration.

In the tropics over the Maritime Continent, middle America and in the SH tropics/subtropics we find a large number of backtraces which end around the tropopause. These all stem from moderate to high amplitude events. Comparing the locations to precipitation indicates that the source is convective excitation. The match to convection is improved if the propagation time of up to two days is taken into account.

The results indicate that ECMWF captures only a certain aspect of the convective forcing, that is excitation by wind shear above a displaced tropopause (moving mountain model, (*Pfister et al.*, 1993)). The absence of fast waves forced directly by the latent heat release of the deep convection is likely due to the fact that the convection parameterization compensates updrafts and downdrafts internally, hence does not couple properly to the dynamical fields of the model but only introduces small net effects.

The cases shown demonstrate that the combination of ray-tracing with 3D measurements facilitates direct interpretation of the results. For current satellites only a complicated interplay between forward modeling and comparison to the data could lead to a similar interpretation, but with much larger uncertainties.

11 Task 8: validation

The task reviews all measurement techniques so far employed for deducing GW momentum flux. It needs to be mentioned here that there was also rapid progress for inferring GW parameters from in-situ and ground-based instrumentation. An overview is presented in table 3.

A suitable location for validation should match the following three criteria:

- A good likelihood for high amplitude GWs
- Moderate variability due to planetary wave structures
- A “natural” high density of scientific instrumentation as well as available campaign infrastructure in order to keep required funding affordable

The study recommends to perform the campaign in winter in Scandinavia.

In order to widen the observational filter and to reduce associated errors the study suggests to use data assimilation for combining the measurements into a mesoscale model. To our knowledge, such an assimilation for GW interpretation is unprecedented. Experience will be gained by using observing system simulation experiments (OSSEs, cf. *Masutani et al.* (2010)) as well as undertaking campaigns.

Finally, data assimilation of global observations guiding the background wind and temperature structures can provide a complementary approach toward extraction of acceleration information. The comparison of these values to GW accelerations calculated from vertical gradients of PREMIER NX-GWMF offers a large potential for scientific studies.

Table 3: Overview of measurement techniques employed for GW research, measured quantities, potential and limitations

	amplitudes T′	hor. wavelength	vert. wavelength	MF from $(T')^2$	MF from $(u_h')^2$	MF from $u_h'w'$	comment
Radiosondes	direct	via dispersion relation	< 10 km	possible	standard (from u′ and T′)	reliable only for large-amplitude waves	
Rocketsonde	direct	via dispersion relation	< 10 km	possible	as for radiosondes	-	
Research Aircraft	direct	-	-	-	-	+ (directional MF)	Needs a high-altitude research aircraft (as Geophysika)
Super-pressure balloon	direct	not done yet, but no theoretical restriction	not done yet, but no theoretical restriction			+ (directional MF)	@ ~ 20 km
Radar	-	via hodograph, 0.5-15 h period	direct, 1-10 km	-	+	+	altitudes $<$ 15-20km
Lidar	direct	-	$>$ 1.5 km depending on altitude	needs hor. wavelength	with wind lidar	with wind lidar	
Nadir	from radiances	$>$ 30 km	$>$ 10 km	possible on events	-	-	small spectral overlap with PREMIER measurements
New instruments							
GLORIA	direct	100 km	3 - 15 km	possible on events			
Not applicable							
Airglow Imager							Altitudes higher than PREMIER observations
GPS Radio Occultations							No GW MF, except on specific satellite constellation configuration

12 Recommendations for further studies

The study provides a successful proof of concept. The inferred level of accuracy matches to the requirements inferred in section 3.1 and which are needed for a significant scientific progress in the field. The ray-tracing task further demonstrates the huge potential of such an unprecedented and unparalleled data set for scientific investigations. However, the study also made evident that substantial work has to be still done if the PREMIER mission is selected.

Retrievals

- Complete processing of four weeks of ECMWF scenario data required a significant amount of computer time simply due to the large amount of simulated measurement data. Further optimization of the tomographic retrieval system will be necessary to continuously process real data at a later stage. Several such optimizations are currently under development at FZJ (e.g. *Ungermann et al.*, 2011; *Ungermann*, 2012).
- Regularization parameters for the retrieval should be further optimized to find the best trade-off between spatial resolution and retrieval noise. However, it needs to be considered that regularization also provides stability for the numerical inversion process.
- The selection of spectral micro-windows is currently based on 1D linear error simulations. 2D error analysis carried out during the course of the study indicated that the 1D error estimates cannot be transferred to 2D. Further attention should be given to 2D retrieval tests with different micro-window settings.

Detrending

A space-time spectral analysis should be employed to subtract the background atmosphere. This requires the generation of a fully time-dependent test data set.

Validation and scientific interpretation

More steps in the direction of the assimilation of different measurement techniques into a mesoscale model should be taken. This could be tested in observing system simulation experiments (OSSEs) as well as for real campaigns. For instance the MAARSY radar and the GLORIA airborne limb imager have the potential to provide 3D wind (MAARSY) and temperature (GLORIA) fields suited for test evaluations.

References

Alexander, M. J., M. Geller, C. McLandress, S. Polavarapu, P. Preusse, F. Sassi, K. Sato, S. Eckermann, M. Ern, A. Hertzog, Y. Kawatani, M. Pulido, T. A. Shaw, M. Sigmond, R. Vincent and S. Watanabe, Recent developments in gravity-wave effects in climate models and the global distribution of gravity-wave momentum flux from observations and models, *Q. J. R. Meteorol. Soc.*, 136, 1103–1124, 2010.

Alexander, M. J., J. Gille, C. Cavanaugh, M. Coffey, C. Craig, T. Eden, G. Francis, C.Halvorson, J. Hannigan, R. Khosravi, D. Kinnison, H. Lee, S. Massie, B. Nardi, J. Barnett, C. Hepplewhite, A. Lambert and V. Dean, Global estimates of gravity wave momentum flux from high resolution dynamics limb sounder (HIRDLS) observations, *J. Geophys. Res.*, 113, 2008.

Ern, M. and P. Preusse, Gravity wave momentum flux spectra observed from satellite in the summertime subtropics: Implications for global modeling, *GEOPHYSICAL RESEARCH LETTERS*, 39, 2012, ISSN 0094-8276.

Ern, M., P. Preusse, M. J. Alexander and C. D. Warner, Absolute values of gravity wave momentum flux derived from satellite data, *J. Geophys. Res.*, 109, 2004.

Ern, M., P. Preusse, J. C. Gille, C. L. Hepplewhite, M. G. Mlynczak, J. M. Russell III and M. Riese, Implications for atmospheric dynamics derived from global observations of gravity wave momentum flux in stratosphere and mesosphere, *J. Geophys. Res.*, 116, 2011.

Fetzer, E. J. and J. C. Gille, Gravity wave variances in LIMS temperatures, I, variability and comparison with background winds, *J. Atmos. Sci.*, 51, 2461–2483, 1994.

Fritts, D. C., Gravity wave saturation in the middle atmosphere: A review of theory and observations, *Rev. Geophys.*, 22, 275–308, 1984.

Fritts, D. C. and M. J. Alexander, Gravity wave dynamics and effects in the middle atmosphere, *Rev. Geophys.*, 41, 2003.

Kim, Y.-H., H.-Y. Chun, P. Preusse, M. Ern and S.-Y. Kim, Gravity wave reflection and its influence on the consistency of temperature- and wind-based momentum fluxes simulated above typhoon Ewiniar, *Atmos. Chem. Phys. Discuss.*, 12, 6263–6282, 2012.

Kim, Y. J., S. D. Eckermann and H. Y. Chun, An overview of the past, present and future of gravity-wave drag parameterization for numerical climate and weather prediction models - Survey article, *Atmosphere-Ocean*, 41, 65–98, 2003.

Lane, T. P. and J. C. Knievel, Some Effects of Model Resolution on Simulated Gravity Waves Generated by Deep Mesoscale Convection, *J. Atmos. Sci.*, 62, 3408–3419, 2005.

Lehmann, C. I., Y.-H. Kim, P. Preusse, H.-Y. Chun, M. Ern and S. Y. Kim, Consistency between Fourier transform and small-volume few-wave decomposition for spectral and spatial variability of gravity waves above a typhoon, *Atmos. Meas. Tech.*, 5, 1637–1651, 2012, ISSN 1867-1381.

Masutani, M., T. W. Schlatter, R. M. Errico, A. Stoffelen, E. Andersson, W. Lahoz, J. S. Woollen, G. D. Emmitt, L.-P. Riishojgaard and S. J. Lord, Observing System Simulation Experiments, in Lahoz, W and Khattatov, B and Menard, R, Editor, *DATA ASSIMILATION: MAKING SENSE OF OBSERVATIONS*, Pages 647–679, SPRINGER-VERLAG BERLIN, HEIDELBERGER PLATZ 3, D-14197 BERLIN, GERMANY, 2010, ISBN 978-3-540-74702-4.

McLandress, C., On the importance of gravity waves in the middle atmosphere and their parameterization in general circulation models, *J. Atmos. Terr. Phys.*, 60, 1357–1383, 1998.

Pfister, L., S. Scott, M. Loewenstein, S. Brown and M. Legg, Mesoscale Disturbances in the Tropical Stratosphere Excited by Convection: Observations and Effects on the Stratospheric Momentum Budget., *J. Atmos. Sci.*, 50, 1058–1075, 1993.

Preusse, P., A. D. Doernbrack, S. D. Eckermann, M. Riese, B. Schaeler, J. Bacmeister, D. Broutman and K. U. Grossmann, Space based measurements of stratospheric mountain waves by CRISTA, 1. Sensitivity, analysis method and a case study, *J. Geophys. Res.*, 107, 2002.

Preusse, P., S. D. Eckermann and M. Ern, Transparency of the atmosphere to short horizontal wavelength gravity waves, *J. Geophys. Res.*, 113, 2008.

Pulido, M. and J. Thuburn, Gravity-wave drag estimation from global analyses using variational data assimilation principles. I: Theory and implementation, *Q. J. R. Meteorol. Soc.*, 131, 1821–1840, 2005.

Pulido, M. and J. Thuburn, Gravity-wave drag estimation from global analyses using variational data assimilation principles. II: Case study, *Q. J. R. Meteorol. Soc.*, 132, 1527–1543, 2006.

Ungermann, J., Improving retrieval quality for airborne limb-sounders by horizontal regularisation, *Atmospheric Measurement Techniques Discussions*, 5, 6577–6626, 2012.

Ungermann, J., J. Blank, J. Lotz, K. Leppkes, L. Hoffmann, T. Guggenmoser, M. Kaufmann, P. Preusse, U. Naumann and M. Riese, A 3-D tomographic retrieval approach with advection compensation for the air-borne limb-imager GLORIA, *Atmos. Meas. Tech.*, 4, 2509–2529, 2011.